Supporting Information Table 1. Scalar couplings measured with the H1C1C2 experiment for helix-35.[a]

	JC1’-H1’	JC2’-H2’	JC1’-H2’	JC2’-H1’	JH1’-H2’ [b]
G738	176.68 ± 0.10	158.22 ± 0.09	2.42 ± 0.10	-1.50 ± 0.09	0.79 ± 0.16
G739	176.33 ± 0.07	157.90 ± 0.07	2.86 ± 0.07	-1.85 ± 0.07	0.67 ± 0.12
C740	180.45 ± 0.07	159.72 ± 0.06	1.70 ± 0.07	-2.14 ± 0.06	1.07 ± 0.12
U741	179.91 ± 0.08	158.90 ± 0.07	2.11 ± 0.08	-2.43 ± 0.07	0.78 ± 0.13
A742	175.54 ± 0.08	157.02 ± 0.08	2.33 ± 0.08	-1.98 ± 0.08	1.02 ± 0.14
A743	175.86 ± 0.07	157.54 ± 0.06	2.76 ± 0.07	-1.78 ± 0.06	0.94 ± 0.12
U744	178.71 ± 0.12	158.81 ± 0.11	1.60 ± 0.12	-2.63 ± 0.11	0.93 ± 0.21
G745	173.44 ± 0.20	157.27 ± 0.24	1.13 ± 0.20	-2.28 ± 0.24	1.73 ± 0.39
U747	173.97 ± 0.21	157.78 ± 0.28	0.14 ± 0.21	-2.46 ± 0.28	3.32 ± 0.40
G748	168.51 ± 0.28	151.37 ± 0.34	-1.29 ± 0.28	-3.28 ± 0.34	4.24 ± 0.50
A749	168.65 ± 0.16	158.10 ± 0.20	-0.93 ± 0.16	-2.45 ± 0.20	3.84 ± 0.31
A750	171.60 ± 0.80	157.25 ± 2.50	-2.28 ± 1.00	-1.48 ± 0.93	5.36 ± 2.10
A751	170.32 ± 0.42	153.30 ± 0.52	0.50 ± 1.00	-3.44 ± 0.44	3.75 ± 0.90
A752	171.10 ± 1.04	153.02 ± 1.36	1.00 ± 2.00	-1.96 ± 0.57	2.37 ± 2.00
A753	175.94 ± 0.70	155.85 ± 0.91	2.13 ± 0.50	-3.40 ± 0.30	1.88 ± 0.64
U754	179.98 ± 0.08	158.96 ± 0.08	2.24 ± 0.08	-2.81 ± 0.08	0.89 ± 0.14
U755	178.89 ± 0.08	158.54 ± 0.08	2.03 ± 0.08	-2.76 ± 0.08	1.22 ± 0.13
A756	175.14 ± 0.12	157.18 ± 0.13	2.14 ± 0.12	-1.74 ± 0.13	1.23 ± 0.21
G757	175.57 ± 0.07	157.76 ± 0.06	2.85 ± 0.07	-2.32 ± 0.06	0.84 ± 0.11
C758	179.61 ± 0.07	158.97 ± 0.06	1.96 ± 0.07	-2.31 ± 0.06	0.84 ± 0.11
C759	180.00 ± 0.06	158.55 ± 0.06	1.92 ± 0.06	-2.67 ± 0.06	0.82 ± 0.10
C760	174.88 ± 0.04	155.89 ± 0.03	0.54 ± 0.04	-2.60 ± 0.03	1.78 ± 0.05

[a] All values in Hertz.

[b] Reported values have been divided by 0.8 to correct for change in H2′ spin state during the final Rance-Kay transfer.

Supporting Information Table 2. Dipolar couplings measured with the H1C1C2 experiment for helix-35.[a]

	DC1’-H1’	DC2’-H2’	DC1’-H2’	DC2’-H1’	DH1’-H2’ [b]
G738	-29.8 ± 0.2	12.1 ± 0.1	1.1 ± 0.2	-4.9 ± 0.1	-4.5 ± 0.2
G739	-37.0 ± 0.2	11.3 ± 0.1	-0.9 ± 0.2	-3.9 ± 0.1	-5.8 ± 0.1
C740	-34.2 ± 0.1	8.3 ± 0.1	-2.2 ± 0.1	-4.0 ± 0.1	-8.2 ± 0.1
U741	-21.8 ± 0.1	0.8 ± 0.1	-2.6 ± 0.1	-3.7 ± 0.1	-9.4 ± 0.1
A742	-12.4 ± 0.2	-1.1 ± 0.1	-3.1 ± 0.2	-4.2 ± 0.1	-9.7 ± 0.2
A743	-4.5 ± 0.1	-5.4 ± 0.1	-4.0 ± 0.1	-5.0 ± 0.1	-10.9 ± 0.1
U744	1.0 ± 0.2	-1.2 ± 0.2	-4.1 ± 0.2	-4.8 ± 0.2	-9.3 ± 0.2
G745	-2.2 ± 0.4	8.7 ± 0.3	-3.5 ± 0.4	-4.9 ± 0.3	-6.7 ± 0.5
U747	-4.9 ± 0.4	13.1 ± 0.4	0.2 ± 0.4	-3.7 ± 0.4	-3.2 ± 0.4
G748	4.6 ± 0.6	-3.0 ± 0.5	0.6 ± 0.6	-2.0 ± 0.5	-2.9 ± 0.6
A749	7.9 ± 0.3	-6.6 ± 0.3	-1.3 ± 0.3	-1.5 ± 0.3	-2.0 ± 0.3
A750	3.8 ± 3.0	-4.7 ± 3.5	-1.1 ± 1.5	-1.9 ± 1.0	-3.5 ± 2.5
A751	-0.5 ± 0.6	4.8 ± 1.5	-2.1 ± 1.5	-1.0 ± 0.7	-3.9 ± 1.0
A752	-15.1 ± 1.7	7.8 ± 1.6	2.7 ± 3.3	-3.9 ± 1.7	-0.7 ± 2.2
A753	-23.5 ± 1.3	5.0 ± 2.0	-2.4 ± 1.5	-3.4 ± 1.1	-8.6 ± 2.0
U754	-17.8 ± 0.2	-9.7 ± 0.1	-4.5 ± 0.2	-4.2 ± 0.1	-10.3 ± 0.2
U755	-6.7 ± 0.1	-3.4 ± 0.1	-4.7 ± 0.2	-3.5 ± 0.1	-10.4 ± 0.2
A756	-0.3 ± 0.2	6.2 ± 0.2	-3.7 ± 0.3	-5.4 ± 0.2	-9.2 ± 0.2
G757	-0.5 ± 0.1	13.6 ± 0.1	-3.1 ± 0.2	-5.0 ± 0.1	-8.1 ± 0.1
C758	-3.2 ± 0.1	13.5 ± 0.1	-0.9 ± 0.2	-4.9 ± 0.1	-6.0 ± 0.1
C759	-8.5 ± 0.1	13.6 ± 0.1	-0.6 ± 0.1	-4.4 ± 0.1	-5.9 ± 0.1
C760	-9.0 ± 0.1	20.6 ± 0.1	-1.5 ± 0.1	-4.4 ± 0.1	-4.1 ± 0.1

[a] All values in Hertz.

[b] Reported values have been divided by 0.8 to correct for change in H2′ spin state during the final Rance-Kay transfer.

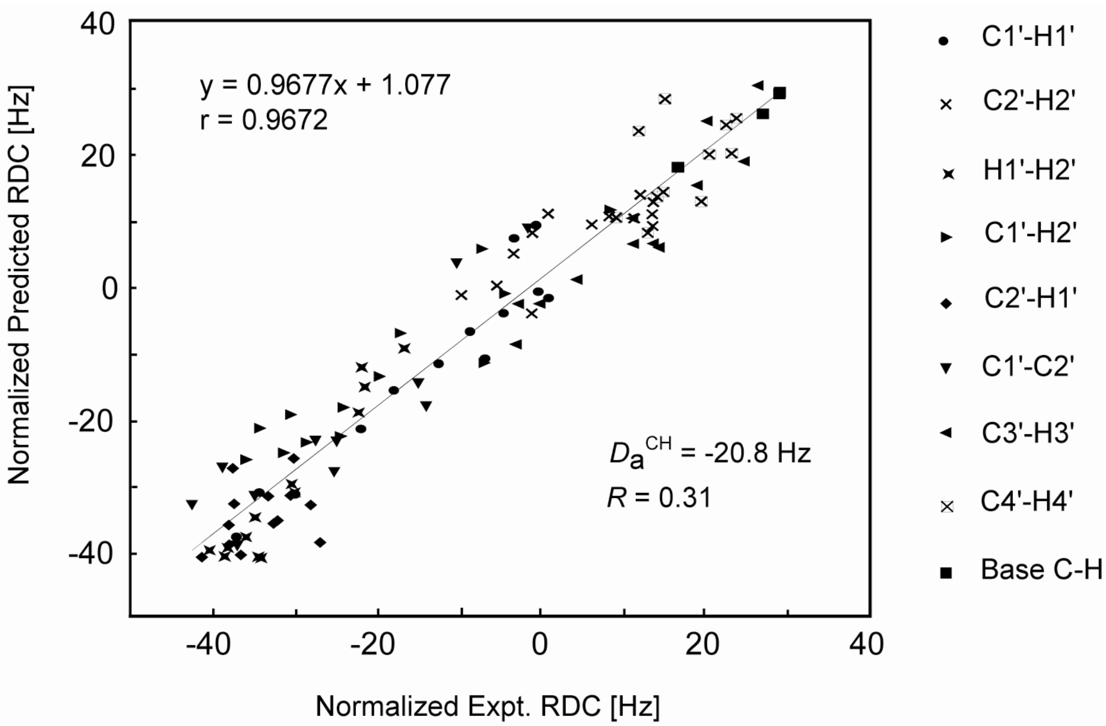

Supporting information Figure 1*:* Correlation plot of normalized predicted RDCs measured for the 12 nucleotides comprising the stem region of helix-35$^{\psi746}$ RNA (G738-A743 and C759-U754) *vs* experimental couplings obtained from an SVD fit of the data to the 1QCU structure. Also included in the fit are four one-bond carbon-proton base RDCs (C8-H8 for A756, G757; C6-H6 for C740, U741) for nucleotides that matched the base type of the 36-fold averaged X-ray structure oligomer, modeled as a repeat of 18 GC basepairs (Klosterman, P. S., Shah, S. A., Steitz, T. A., Biochemistry 38, 14784,1999).

Note: A labelling error in the scale of the above plot has been corrected in this version of the Supporting Information.

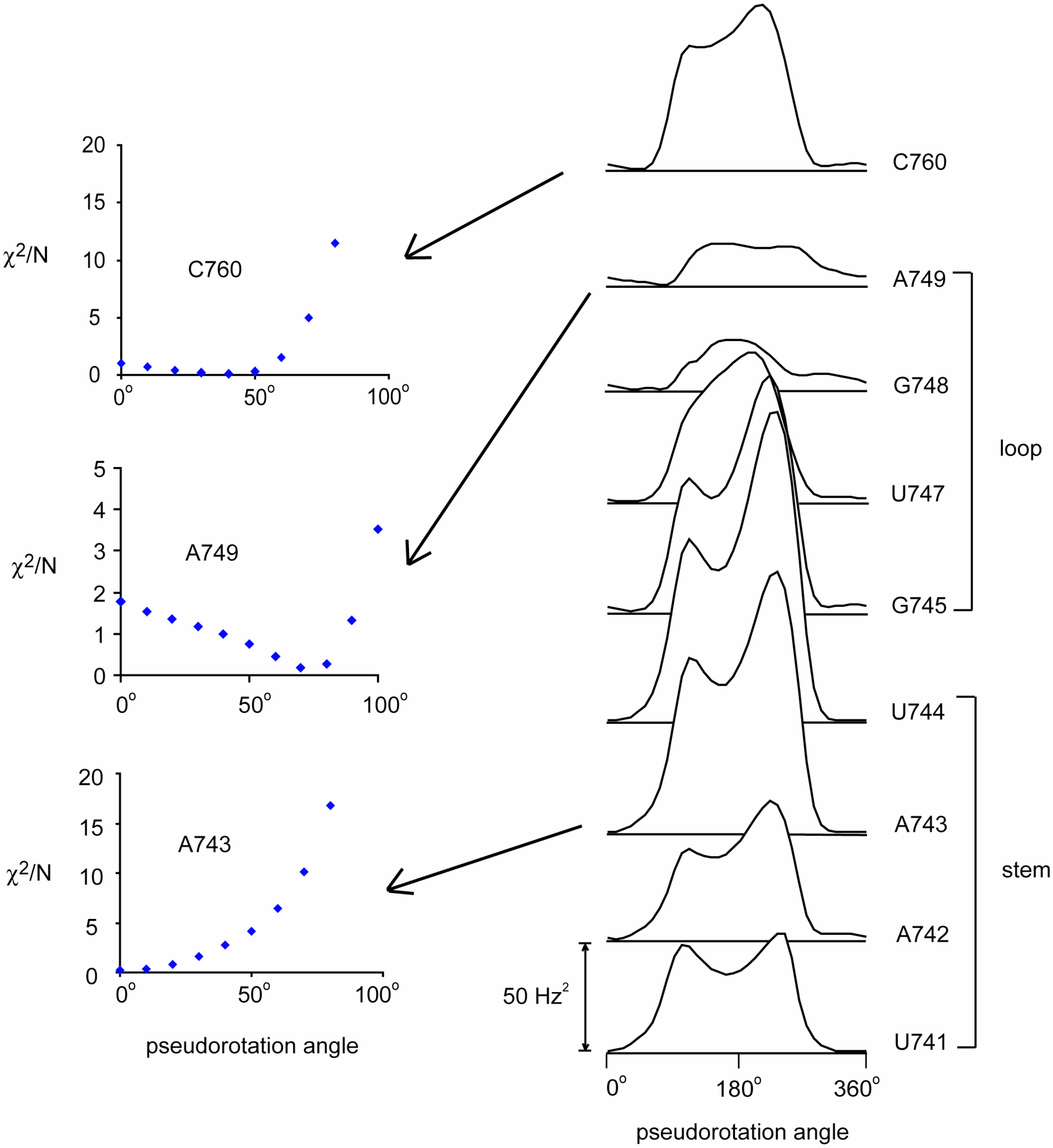

Supporting Information Figure 2. Residual of the SVD fit (χ^2/N) between normalized experimental D(C1'H1'), D(C2'H2'), D(C3'H3'), D(C4'H4'), D(C1'H2'), D(C2'H1'), D(H1'H2') and D(C1'C2') dipolar couplings and values best fitted for a ribose with a pucker amplitude of 35°, as a function of the pseudorotation phase angle, for representative stem and loop residues of Helix-35ψ^{746}. Expanded regions are shown on the left for A743, A749, and C760.

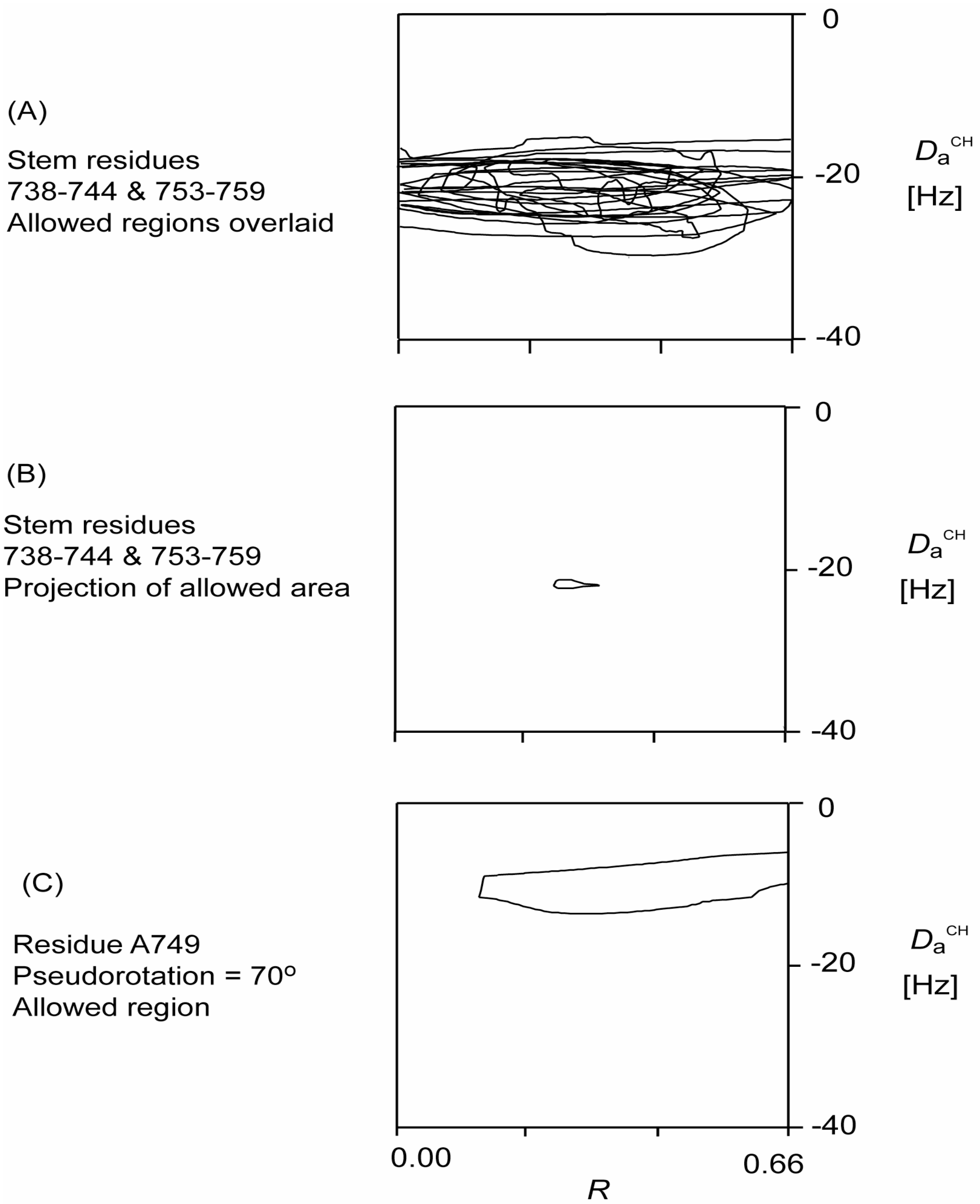

Supporting Information Figure 3. Contour plots of systematic (D_a^{CH},R) grid search results, where experimental dipolar couplings are best fitted to (A,B) a C3'-endo ribose (in all cases allowing the orientation of the alignment tensor to vary during the fit, but keeping D_a^{CH} and R fixed), and (C) to a ribose with a pseudorotation phase of 70° and a pucker amplitude of 35°. (A) Superposition of the contours that mark (D_a^{CH},R) regions, where a fit within experimental error can be obtained for all 12 stem riboses. (B) Projection of the 12 superimposed grid search results of panel (A), displaying the common (D_a^{CH},R) region where all 12 riboses can simultaneously satisfy the dipolar couplings to within experimental error. (C) Results for loop nucleotide A749, indicating a much reduced D_a^{CH} and a relatively poorly defined P. All contours are drawn at $\chi^2/N = 4$ Hz^2, i.e., assuming a 2 Hz random error in the normalized couplings.